HAL
open science

Extreme Values, Heavy Tails and Linearization Effect : a Contribution to Empirical Multifractal Analysis

Patrice Abry, Vladas Pipiras, Herwig Wendt

To cite this version:

Patrice Abry, Vladas Pipiras, Herwig Wendt. Extreme Values, Heavy Tails and Linearization Effect : a Contribution to Empirical Multifractal Analysis. GRETSI 2007, Université de technologie de Troyes (UTT) ; Université de Reims Champagne-Ardennes (URCA), Sep 2007, Troyes, France. ensl-00160153

HAL Id: ensl-00160153

https://ens-lyon.hal.science/ensl-00160153v1

Submitted on 5 Jul 2007

HAL is a multi-disciplinary open access archive for the deposit and dissemination of scientific research documents, whether they are published or not. The documents may come from teaching and research institutions in France or abroad, or from public or private research centers.

L'archive ouverte pluridisciplinaire **HAL**, est destinée au dépôt et à la diffusion de documents scientifiques de niveau recherche, publiés ou non, émanant des établissements d'enseignement et de recherche français ou étrangers, des laboratoires publics ou privés.

Extreme Values, Heavy Tails and Linearization Effect: A Contribution to Empirical Multifractal Analysis

Patrice ABRY[1], Vladas PIPIRAS[2], Herwig WENDT[1]

[1]Laboratoire de Physique, UMR 5672, CNRS, Ecole Normale Supérieure de Lyon,
46, allée d'Italie, 69364 Lyon cedex 7, France, Tel: 33 47272 8493,

[2]Dept. of Statistics and Operational Research, UNC-CH, Chapel Hill, NC 27599, USA.
The CNRS Support for the visiting researcher position of V. Pipiras is gratefully acknowledged.
V. Pipiras is supported in part by the NSF grant DMS-0505628
patrice.abry@ens-lyon.fr, pipiras@email.unc.edu, herwig.wendt@ens-lyon.fr

Résumé – L'analyse multifractale devient un outil classique de traitement du signal communément utilisé pour des tâches usuelles telles que détection, identification ou classification. En pratique, elle consiste essentiellement en la mesure d'exposants de lois d'échelle. Il a longtemps été considéré que ces exposants s'identifiaient exactement à ceux impliqués dans le détail de la construction multiplicative de la plupart des processus multifractals connus ou utilisés. Il a cependant été observé récemment que ces exposants de lois d'échelle présentent nécessairement un comportement linéaire en fonction de l'ordre statistique q, dans la limite des grands q. Cette association abusive est à l'origine d'interprétations erronées des exposants mesurés sur des données réelles. Le présent article contribue à l'analyse et à la contribution de cet effet de linéarisation et ainsi à la clarification de cette association incorrecte. Il indique notamment que l'effet de linéarisation peut être relié au caractère *ailes lourdes*, associé par nature aux processus multifractals ainsi qu'à leur structure de dépendance, grâce à un argument impliquant les valeurs extrêmes des fonctions de structure. Ces arguments sont inspectés au moyen de simulations numériques conduites sur des processus multifractals particuliers, les mouvements Poisson composés (CPM).

Abstract – Multifractal analysis is becoming a standard tool in signal processing commonly involved in classical tasks such as detection, estimation or identification. Essentially, in practice, it amounts to measuring a collection of scaling law exponents. It has generally been thought by practitioners that these scaling exponents were related to the details of the multiplicative construction underlying the definitions of most known and used multifractal processes. However, recent results show that these scaling exponents necessarily behave as a linear function of the statistical orders q, for large qs. This confusing association has often been misleading in the use of scaling exponents for real-life data analysis. The present work contributes to the analysis and understanding of this linearization effect and hence to a clarification of this improper association. It is shown that this effect can be explained through an argument involving extreme values and the intrinsic heavy tail nature of the marginal distributions and dependence structure of multifractal processes. These issues are analyzed by means of numerical simulations conducted over specific multifractal processes, the compound Poisson motions (CPM).

1 Position of the problem

Multifractal analysis provides a well-grounded mathematical theory and well-established analysis tools for scaling, or scale invariant, data encountered in many different applications. It is based on the structure function

$$S_n(q,a) = \frac{1}{n_a}\sum_{k=1}^{n_a} |T_X(a,ak)|^q, \qquad (1)$$

where $T_X(a,t) = X(t+a) - X(t)$ are the increments of the data under analysis $X(t)$ at scale a, n is the sample size of $X(t)$ and $n_a = n/a$. Essentially, multifractal analysis states that

$$S_n(q,a) \simeq c_q a^{\zeta(q)}, \quad \text{as } a \to 0. \qquad (2)$$

Estimating $\zeta(q)$, known as the scaling exponents, is the goal of empirical multifractal analysis. Estimation is commonly performed by linear fits in log-log plots. The estimates of these scaling exponents $\zeta(q)$ are then involved in standard signal processing tasks such as detection, identification or classification.

Despite the above procedure being widely used in practice, the behavior and statistical performance of the estimates of scaling exponents remain poorly analyzed and understood, which sometimes leads to misinterpretation of the results, yielded by the estimated exponents. To contribute to a better understanding of these procedures, we consider here a particular class of multifractal processes known as Compound Poisson Motions (CPM) [2]. CPM are chosen because their increments $\{T_X(a,t), t \in \mathbb{R}\}$ form stationary processes, for each analysis scale a. It can be further shown [3] that

$$\mathbb{E}|T_X(a,t)|^q \simeq C_q a^{\lambda(q)}, \quad \text{as } a \to 0, \qquad (3)$$

for $0 < q < q_c^+ = \sup\{q : E|T_X(a,t)|^q < \infty\}$, where $\lambda(q)$ depends on the specific details of the CPM construction.

Since sample averages are naturally used as estimates for the ensemble averages, it has long and largely been believed in the applied multifractal literature that the functions $\zeta(q)$ and $\lambda(q)$ in (2) and (3) were identical, at least for $0 < q \le q_c^+$. However, after the seminal works of Molchan [10], Ossiander & Waymire [12] on Mandelbrot multiplicative cascades [7], it is now being realized that the two functions $\lambda(q)$ and $\zeta(q)$ coincide, surprisingly, only on the narrow range of powers $0 < q \le q_*^+$ with $q_*^+ < q_c^+$. Moreover, $\zeta(q)$ is known to behave as a linear function for $q > q_*^+$ (referred to as the linearization effect). These observations have been confirmed in

a comprehensive empirical study by Lashermes et al. [6] who conjectured that this phenomenon is intrinsic to all multifractal processes and measures. In a number of significant contributions, whose most prominent are [8] and [9] (Chapter 9), Mandelbrot relates negative singularity observation and *super-sampling* issues, intimately tied to the the linearization effect, to the intrinsically heavy tail nature of multiplicative cascades. The present contribution aims at contributing to a better understanding of the origins and causes of the differences in nature of these two different functions of q: $\lambda(q)$ and $\zeta(q)$.

2 Compound Poisson Motion

Compound Poisson cascade. Compound Poisson cascades (CPC) are defined by Barral & Mandelbrot [2] as

$$Q_r(t) = C \prod_{(t_i,r_i)\in\mathcal{C}_r(t)} W_i, \quad r > 0, \tag{4}$$

where $\mathcal{C}_r(t) = \{(t',r') : r \le r' \le 1, t - r'/2 \le t' \le t + r'/2\}$ is a cone, (t_i, r_i) are random points of a Poisson measure on a rectangle $I = \{(t',r') : r \le r' \le 1, -1/2 \le t' \le T + 1/2\}$ having intensity measure $dm(t,r)$, W_i are positive i.i.d. multipliers associated with points (t_i, r_i), and $C = C(r,t)$ is a normalizing constant such that $\mathbb{E}Q_r(t) = 1$. It can be shown that CPC satisfy the following key resolution equation:

$$\mathbb{E}Q_r(t)^q = \exp - (\varphi(q) m(\mathcal{C}_r(t))),$$

with $\varphi(q) = c((1 - \mathbb{E}W^q) - q(1 - EW))$ (c being an arbitrary positive constant) and $m(\mathcal{C}_r(t)) = \int_{\mathcal{C}_r(t)} dm(t',r')$.

Compound Poisson motion. On condition that $\varphi(1^-) \ge -1$, compound Poisson motion (CPM) is a well-defined process:

$$A(t) = \lim_{r\to 0} \int_0^t Q_r(s) ds. \tag{5}$$

Finiteness of moments and heavy tails. It has been shown [2] that the moments of $T_A(a,t) = A(t+a) - A(t)$ are finite only up to order $0 < q < q_c^+ = \sup\{q \ge 1, q + \varphi(q) - 1 \ge 0\}$. One then expects that $P(T_A(a,t) \ge x) \sim x^{-q_c^+}$, when $x \to +\infty$ and hence that the variables $T_A(a,t)$ are heavy-tailed.

Stationary Increments. If $dm(t,r) = g(r)drdt$, the increments $T_A(a,t)$ of A are stationary [3].

Scaling properties. In addition, when $g(r)dr = c(dr/r^2 + \delta_{\{1\}}(dr))$ (as proposed in [1]), where $\delta_{\{1\}}(dr)$ denotes a point mass at $r = 1$, $A(t)$ exhibits scaling properties of the form of Eq. (3), with $\lambda(q) = q + \varphi(q)$, for $0 < q < q_c^+$ [3].

Multifractal properties. From the results proven in [2], we can infer that the multifractal spectrum $D_A(h)$ of A can be derived from the Legendre transform $D_\lambda(h) = \min_{q\neq 0}(1 + qh - \lambda(q))$ of $\lambda(q)$ as

$$D_A(h) = \begin{cases} D_\lambda(h), & \text{if } D_\lambda(h) \ge 0, \\ -\infty, & \text{otherwise.} \end{cases} \tag{6}$$

The quantity $D_A(h)$ is the Hausdorff dimension of the set of time points $t \in \mathbb{R}$ where the sample path can be characterized with the singularity (or Hölder) exponent h:

$$|T_A(a,t)| \simeq c|a|^h, \quad \text{as } a \to 0. \tag{7}$$

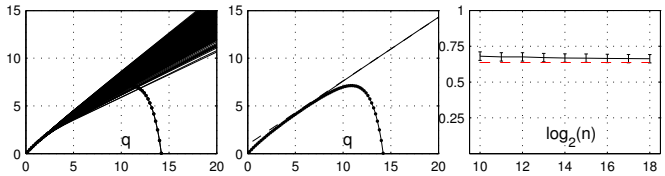

Figure 1: **Linearization effect.** $\widehat{\zeta}(q)$ versus q, observed over 1000 realizations (left) and averaged over all realizations (middle), together with the curve $\lambda(q)$ (solid dotted curve), the dashed line expands the linear behavior observed at large q. Right: averaged slope, characterizing this linear behavior, as a function of $\log_2 n$. Observe that it does not depend on n and is found to be very close to $h_*^+ \simeq 0.64$ (dashed - red - line).

The multifractal spectrum $D_A(h)$ hence provides a *global* description of the *local* fluctuations of a sample path of A. For a thorough introduction to multifractal analysis, the reader is referred to e.g., [5].

3 Empirical multifractal formalism

Multifractal formalism. Empirical multifractal analysis aims at estimating the multifractal spectrum of a process from a given observed sample path. This is commonly performed by computing structure functions, as in Eq. (1), based on increments. Such structure functions are assumed to exhibit power law behaviors as in Eq. (2). The so-called multifractal formalism states that the Legendre transform $D_\zeta(h)$ of the corresponding scaling exponents $\zeta(q)$ yields a convex hull of D_A: $D_\zeta(h) \ge D_A(h)$. In the case of CPM, this turns to an equality.

Estimation procedures. Estimation of the scaling exponents $\zeta(q)$ is commonly conducted through the linear regression of the log of the structure function $S_n(q,a)$ in (1) over dyadic scales $a_j = 2^{j_1}, \ldots, 2^{j_2}$ (throughout this text, $\sum$ stands for $\sum_{j=j_1}^{j_2}$, the weights w_j satisfy $\sum w_j = 0$ and $\sum j w_j = 1$):

$$\widehat{\zeta}(q) = \sum w_j \log_2 S_n(q, 2^j). \tag{8}$$

4 Linearization effect

Numerical simulations. All numerical simulations reported below were conducted over $R = 1000$ independent realizations of CPM, with various $\varphi(q)$ and various data lengths ($n = 2^{10}, \ldots, 2^{18}$), within a single integral scale. Plots and results are presented for a specific $\varphi(q)$ (based on lognormal multipliers W) yielding numerically $q_*^+ \simeq 6.8$, $h_*^+ \simeq 0.64$ and $q_c^+ \simeq 13.8$. However, the results presented here hold for all choices of $\varphi(q)$.

Linearization effect. The estimation procedure (8) has been applied to R realizations of CPM. First, we observe that, for each and every realization of CPM, $\widehat{\zeta}(q)$ is close to $\lambda(q)$ at small qs, i.e., $0 \le q \le q_n$ while it behaves linearly in q, for large qs, i.e., $\widehat{\zeta}(q) = \alpha_n + \beta_n q$, for $q \ge q_n$, where α_n, β_n and q_n are RVs whose means are found not to depend on n [6]. This is illustrated in Fig. 1, left plot. Second, averaging over the R realizations, we observe (Fig. 1, middle plot) that $\langle\widehat{\zeta}(q)\rangle_R$ is close to $\lambda(q)$ at small qs but behaves linearly in q, at

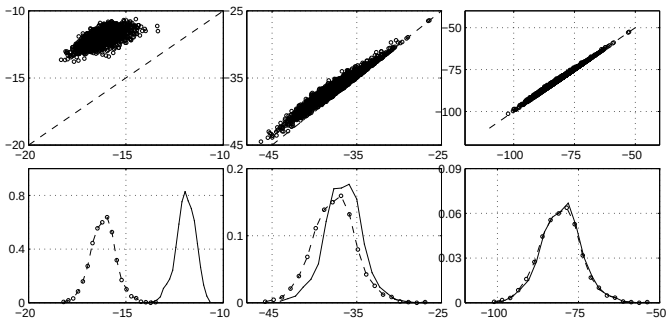

Figure 2: **Structure functions versus extrema.** Two sides of Relation (12): Scatter plots (top row) and empirical PDFs (bottom row), for $j = 5$ with (left to right) $q = 2, 7(\simeq q_*^+), 20$.

large qs. Third, we observe that the slope and intercept of this average linear behavior do not vary (or only extremely slowly vary) when n is increased (estimated slopes as a function of n are reported in Fig. 1, right plot). Such observations can be gathered as follows: $\langle\widehat{\zeta}(q)\rangle_R \simeq \zeta(q)$, where

$$\zeta(q) = \begin{cases} \lambda(q), & \text{if } q \leq q_*^+, \\ 1 + qh_*^+, & \text{if } q > q_*^+, \end{cases} \tag{9}$$

$$h_*^+ = \min{}_h\{D_A(h) = 0\}, \quad q_*^+ = (dD_A/dh)_{h=h_*^+}. \tag{10}$$

They are referred to in [6] as the *linearization effect* of the scaling exponents. It is worth mentioning again that one necessarily has $q_*^+ \leq q_c^+$, and q_*^+ is often far smaller than q_c^+. The equations above are fully consistent with the results in [10, 12] that were previously obtained for the specific case of Mandelbrot cascades. It is formulated as a general conjecture for multifractal processes in [6]. It can appear paradoxical as ensemble averages (in Eq. (3)) and time averages (in Eq. (1)) differ. The goal of the present work is to contribute to a better understanding of the origins of this linearization effect.

5 Extreme values and heavy tails

Structure functions and extreme values. Simple algebra yields that the structure functions $S_n(q, 2^j)$ are driven by the largest increment at scale $a = 2^j$,

$$M_{n_j}(2^j) = \max\{|T_A(2^j, 2^j k)|,\ k = 1, \ldots, n_j\} \tag{11}$$

for fixed n, in the limit $q \to +\infty : S_n(q, 2^j) \simeq \frac{1}{n_j}(M_{n_j}(2^j))^q$,

$$\text{or, } \log_2 S_n(q, 2^j) \simeq -\log_2 n_j + q \log_2 M_{n_j}(2^j). \tag{12}$$

As mentioned in Section 2, the variables $T_A(a, t)$ have heavy tails. Be they independent, the order q for which $M_{n_j}(2^j)$ takes the control of $S_n(q, 2^j)$ should be such that $T_A(a, t)^q$ has infinite mean (cf. e.g., [4], Chapter 8), i.e., when $q \geq q_c^+$. Fig. 2 illustrates that the relevance of (12) actually starts for $q \simeq q_*^+ \leq q_c^+$.

Extreme value distributions. It is well-known that the distributions of maxima of i.i.d. random variables are modeled by extreme value distributions [4]. In the present study, the variables $T_A(a, t)$ have heavy tails, hence so do the $T_A(a, t)^q$, $q > 0$. Therefore, the maximum taken over *independent* $T_A(a, t_k)$, $k = 1, ..., n_a$, would theoretically follow a Frechet distribution with a power law tail $x^{-q_c^+}$ as $x \to +\infty$ [4]. For a given realization of CPM, the $T_A(a, t_k)^q, k = 1, ..., n_a$, entering the sums $S_n(q, 2^j)$, are, by construction of CPM, dependent so that the limit distribution of their maxima is not theoretically known. Therefore, we chose to fit the distribution of $M_{n_j}(2^j)$, separately at each scale $a = 2^j$, using the generalized extreme value (GEV) probability density distribution, whose cumulative distribution function reads [4]: $F_{\xi,\sigma,\mu}(x) = \exp - \left\{(1 + \xi((x - \mu)/\sigma)^{-1/\xi}\right\}$.

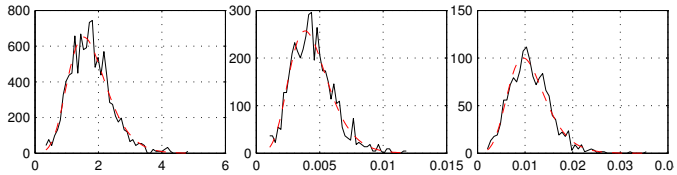

Figure 3: **Extreme values distribution fits.** PDFs of the maxima $M_{n_j}(2^j)$ as in (11) (solid line) and their best GEV fits (dashed lines) for scales $a = 2^j$ with $j = 4, 6, 8$.

Extreme value fits. Fig. 3 clearly indicates a satisfactory agreement between the empirical PDFs of $M_{n_j}(2^j)$ and the GEV distribution. Moreover, Fig. 4 (left plot) shows unambiguously that the estimated parameter ξ depends neither on the scale 2^j nor on the sample number n:

$$\xi_{j,n} \simeq \xi_0. \tag{13}$$

Simple algebra shows that the tail of the GEV probability density function is controlled by the exponent $1/\xi$. The estimated $1/\xi_0$ turns out to be very far from the exponent q_c^+ that would be expected under independence of the $T_A(a, t_k)$ and happens to be consistently close to q_*^+ (cf. Fig. 4, left plot). The empirical PDFs of $T_A(a, t)$ (not shown here for sake of space) also exhibit power law tails, with exponent q_*^+, which is consistent with what is observed for their maxima.
Moreover, Fig. 4 (middle plot) clearly shows that the coefficients $\mu_{j,n}$ and $\sigma_{j,n}$ are characterized by power law behaviors, with respect to the scales 2^j, where the multiplicative factors depend on n, while the power law exponents do not and turn out to be equal to h_*^+, for all n (cf. Fig. 4, right plot):

$$\mu_{j,n} \simeq \mu_{0,n} 2^{jh_*^+}, \quad \sigma_{j,n} \simeq \sigma_{0,n} 2^{jh_*^+}. \tag{14}$$

These findings (Eq. (13) and (14)) are consistent with the analyses recently proposed in [11]. Combined together, the observations above yield:

$$\{M_{n_j}(2^j)\}_{j=j_1,\ldots,j_2} \stackrel{d}{\simeq} \{2^{jh_*^+}(\sigma_{0,n}\Lambda_{\xi_0}^j + \mu_{0,n})\}_{j=j_1,\ldots,j_2}, \tag{15}$$

where each $\Lambda_{\xi_0}^j$ is a random variable drawn from the same $F_{\xi_0,1,0}$ GEV distribution, which does not depend on j.

Linearization effect: slope h_*^+. Combining Definition (8) with empirical results (12) and (15) implies, as $q \to +\infty$,

$$\begin{aligned} \widehat{\zeta}(q) &= \sum w_j \log_2 S_n(q, 2^j) \stackrel{d}{\simeq} -\sum w_j \log_2 n_j \\ &+ qh_*^+ \sum j w_j + q \sum w_j \log_2(\sigma_{0,n}\Lambda_\xi^j + \mu_{0,n}) \\ &\simeq 1 + q\left(h_*^+ + \sum w_j \log_2(\sigma_{0,n}\Lambda_\xi^j + \mu_{0,n})\right), \end{aligned}$$

since $n_j \simeq n2^{-j}$ yields $-\sum_j w_j \log_2 n_j \simeq 1$. In itself, it explains the linearization effect observed for each realization. Moreover, taking the average over realizations yields

$$\langle\widehat{\zeta}(q)\rangle_R \simeq 1 + qh_*^+ + q\sum w_j \langle\log_2(c_{0,n}\Lambda^j + d_{0,n})\rangle_R.$$

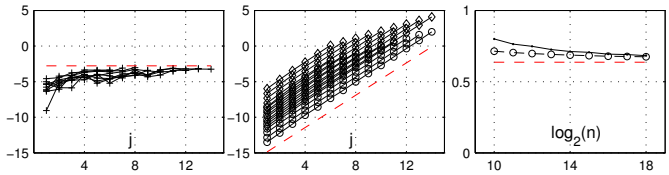

Figure 4: **Extreme value fits and multifractal properties.** $\log_2 \xi_{j,n}$ ('$\diamond$') (left plot) $\log_2 \sigma_{j,n}$ ('o') and $\log_2 \mu_{j,n}$ ('+') (middle plot) versus j, for various n. The horizontal dashed (red) line (left plot) corresponds to $-\log_2 q_*^+$, while the diagonal one (middle plot) has slope h_*^+ (intercept being arbitrary). Right plot: estimated slopes for $\log_2 \sigma_{j,n}$ ('o') and $\log_2 \mu_{j,n}$ ('$\diamond$') do not vary significantly with n and are close to h_*^+ (dashed, red line).

Since $\langle \log_2(\sigma_{0,n}\Lambda_\xi^j + \mu_{0,n})\rangle_R$ does not depend on j and $\sum w_j \equiv 0$, this explains the linearization effect observed as an average over realizations, cf. Eq. (9):

$$\langle \widehat{\zeta}(q)\rangle_R \simeq 1 + qh_*^+. \tag{16}$$

Linearization effect: critical order q_*^+. On the one hand, the empirical results reported above suggest a power law tail behavior $x^{-q_*^+/q}$ for the variables $T_A(a,t)^q$, observed from a single realization and therefore, that they exhibit infinite mean as if when $q \gtrsim q_*^+$. This explains that the maximum $M_{n_j}(2^j)^q$ takes control of the sum $S_n(q, 2^j)$ at q_*^+. On the other hand, we observed in Fig. 1 that $\zeta(q)$ evolves continuously and without discontinuity from $\lambda(q)$ at small qs, to $1 + qh_*^+$ for large qs. This implies and explains the existence of a critical order q_*^+ and defines it as $\lambda(q_*^+) = 1 + q_*^+ h_*^+$. Using the Legendre transform in Eq. (10), this can be rewritten in clear agreement with Definition (10) as well as with the conjecture in [6], as:

$$1 + q_*^+ (d\lambda/dq)_{q=q_*^+} - \lambda(q_*^+) = 0. \tag{17}$$

These two different arguments explain separately that the linearization effect starts to occur when $q \gtrsim q_*^+$.

6 Conclusions and perspectives

Multifractal properties and extreme values. Observations (15), indicating that $M_n(2^j) \simeq C_n 2^{jh_*^+}$, as $a = 2^j \to 0$, where C_n is a suitable random variable, are strikingly consistent with the multifractal paradigm. Indeed, recall from Section 2 that multifractal analysis associates to each time position t an Hölder exponent as $|T_A(a,t)| \simeq c(t)a^{h(t)}$, as $a \to 0$. Then, the largest increments (hence the maxima) are observed in the limit $a \to 0$ for the smallest h, that is where $A(t)$ is the most singular. By Definition (10), such smallest exponent is h_*^+.

Heavy tails, dependence and linearization effect. The analyses reported here show that the existence of the linearization effect is a combined consequence of two major properties of CPM: their increments are heavy-tailed and possess a specific dependence structure resulting from the multiplicative construction.

Perspectives. First, it is conjectured and currently observed in numerical simulations not reported here that the present analyses of the linearization effect holds for all multifractal processes and not only CPM or those resulting from multiplicative constructions (such as the Mandelbrot cascades [7] or infinitely divisible motions [3]). Indeed, multifractal processes will in general gather the two key ingredients mentioned above: heavy tails and a form of time dependence structure, which the multifractal spectrum characterizes in an indirect way. Second, a full and relevant multifractal analysis needs to be based on wavelet leaders [5] rather than on increments and involves both positive and negative qs. It is of interest to understand how these relations between multifractality, heavy tails, dependence, extreme values and linearization effect extend to this more accurate framework and accommodate the negative qs. These two research directions are being currently investigated.

References

[1] E. Bacry and J.F. Muzy. Log-infinitely divisible multifractal processes. *Commun. Math. Phys.*, 236:449–475, 2003.

[2] J. Barral and B. Mandelbrot. Multiplicative products of cylindrical pulses. *Probab. Theory Relat. Fields*, 124:409–430, 2002.

[3] P. Chainais, R. Riedi, and P. Abry. On non scale invariant infinitely divisible cascades. *IEEE Transactions on Information Theory*, 51(3), March 2005.

[4] P. Embrechts, C. Klüppelberg, and T. Mikosch. *Modelling extremal events*. Springer-Verlag, Berlin, 1997.

[5] S. Jaffard. Wavelet techniques in multifractal analysis. In *Fractal Geometry and Applications: A Jubilee of Benoît Mandelbrot, M. Lapidus et M. van Frankenhuijsen Eds., Proceedings of Symposia in Pure Mathematics*, volume 72(2), pages 91–152. AMS, 2004.

[6] B. Lashermes, P. Abry, and P. Chainais. New insights into the estimation of scaling exponents. *Int. J. of Wavelets, Multiresolution and Information Processing*, 2(4):497–523, 2004.

[7] B. B. Mandelbrot. Intermittent turbulence in self similar cascades: Divergence of high moments and dimension of the carrier. *J. Fluid. Mech.*, 62:331, 1974.

[8] B. B. Mandelbrot. Limit lognormal multifractal measures. *Landau Memorial Conference (Tel Aviv, 1988). Edited by E. A. Gotsman et al. New York: Pergamon,*, pages 309–340, 1990.

[9] B. B. Mandelbrot. *Fractals and scaling in finance*. Selected Works of Benoit B. Mandelbrot. Springer-Verlag, New York, 1997. Discontinuity, concentration, risk, Selecta Volume E, With a foreword by R. E. Gomory.

[10] G. M. Molchan. Scaling exponents and multifractal dimensions for independent random cascades. *Comm. Math. Phys.*, 179:681, 1996.

[11] J.F. Muzy, E. Bacry, and A. Kozhemyak. Extreme values and fat tails of multifractal fluctuations. *Phys. Rev. E*, page 066114, 2006.

[12] M. Ossiander and E.C. Waymire. Statistical estimation for multiplicative cascades. *The Annals of Statistics*, 28(6):1533–1560, 2000.